INVESTIGATION OF LARGE SYSTEMS CONSISTING OF MANY SPATIAL POLYHEDRAL BODIES

Beate Muth
Institute B of Mechanics
University of Stuttgart
Germany
muth@mechb.uni-stuttgart.de

Peter Eberhard
Institute B of Mechanics
University of Stuttgart
Germany
eberhard@mechb.uni-stuttgart.de

Abstract

Goal of the work presented here is an investigation of the dynamical behavior of many differently shaped bodies. By means of granular matter simulations large systems like bulk solids, e.g. in silos, or rock that may consist of silicic, or other systems like carriage systems can be investigated. For an efficient simulation of such systems methods from Molecular Dynamics (MD) and Multibody Systems (MBS) are combined.

Simulations of granular material or bulk solids are based on free bodies in space. Therefore, each body has six degrees of freedom and the equations of motion can be obtained easily taking into account three elementary rotations for example the Kardan-angles and three translational degrees of freedom. After neighboring body pairs are found, the very time consuming collision detection for polygonal bodies can be accomplished. In order to check whether there is a collision between two neighboring body pairs, it has to be checked, whether there is a vertex of one body inside the other body. It will be focused also on the calculation of the contact forces in normal and tangential direction.

Key words

Molecular Dynamics, Multibody Systems, Discrete Element Method, Contacts, Collision Detection

1 Introduction

In order to be able to describe the dynamical behavior of systems, which consist of many bodies, very different approaches exist. Systems that consist of rigid bodies can e.g. be described by means of the Multibody Systems (MBS), [Schiehlen, Eberhard, 2004]. Mass point systems can be regarded as a special case of MBS. If flexible bodies are to be examined, the Finite Element Method (FEM) is used frequently, compare [Eberhard, 2000] or the Boundary Element Method (BEM) may be used. Each of these methods has different benefits.

MBS simulations show relatively short computation times, since normally systems consisting of only a few degrees of freedom are regarded. However, deformations of the bodies are usually neglected. On the other hand systems, which are modeled by means of the FEM, possess many degrees of freedom and the equations of motion usually become very large. However, deformations of the bodies can be represented. Also efforts have been made to extend the method of the MBS to flexible bodies see e.g. [Schwertassek, Wallrapp, 1999]. A hybrid MBS/FEM method is presented in [Eberhard, 2000]. There, bodies are modeled during the contact by means of the FEM in order to be able to consider deformations, while all other bodies of the system are regarded as rigid. This attempt, which combines FEM and MBS, can unite the advantages of both methods. However, in the same way as the above mentioned methods, it has the disadvantage that the number of contacting bodies at each time is limited by a feasible computation time.

2 Molecular Dynamics

A very efficient method in order to model granular systems is the Molecular Dynamics (MD) or the Discrete Element Method (DEM). It allows for the efficient examination of motion and contacts of many thousands of particles.

Originally in MD molecules are investigated and it is the goal to describe their interactions and collective dynamical behavior. Interactions between particles depend on measurable characteristics of the materials, e.g. viscosity or elasticity. In order to simulate a high number of bodies, in MD the molecules are often modeled as rigid spheres. The material behavior is then represented by the forces acting on the bodies. In MD such forces may be attractive forces such as van der Waals forces, but also contact forces are investigated. The formulation of the contacting force between the different bodies is based on simple models in order to hold the computation times within an acceptable range. Often,

small overlaps between the bodies are accepted, see e.g. [Luding, 1998]. These forces, which are applied to bodies in MD, are resulting from gravitation and from contacts, e.g. from contacts of the bodies among each other.

In order to determine, whether there is a contact between two bodies, the distance between the bodies has to be detected. Without further considerations, for such a collision detection each body has to be tested against every other body of the system. That means a double loop must be accomplished over the total number of the bodies. Therefore, the necessary calculation time in order to test all body pairs with respect to collision is proportional to n^2 see [Allen, Tildesley, 1989]. This leads to a simulation time of $O(n^2)$. Already in 1967 Verlet [Allen, Tildesley, 1989] suggested a technique in order to improve the calculation times, that are required for collision detection. It has been his idea to search for close body pairs in advance. Therefore, a list for each body has to be produced, consisting of its neighboring bodies, in order to have to perform the collision detection not for each existing pair of bodies of the system, but only for neighboring bodies. Many different neighborhood search methods for the presorting of neighboring body pairs have been developed in order to produce such neighborhood lists. These lists must be updated occasionally, depending on the method that is used. We will briefly describe one such method in Section 4.

3 Multibody System Dynamics

The systems considered here consist of free bodies in space. Such a system holds six degrees of freedom for each body, three translational and three rotational ones. For the rotational degrees of freedom, e.g. the Kardan-angles can be taken into account. All degrees of freedom can be summarized in a vector $\mathbf{y} = [\mathbf{y}_T \ \mathbf{y}_R]^T$ of generalized coordinates. In MBS the equations of motion are often formulated for the whole system. Since here no joints or guidances are considered, the generalized coordinates correspond directly to the unconstrained motion. Therefore, the bodies here are only interdependent due to contact forces and the equations of motion can be formulated for each body separately,

$$\begin{aligned} m_i\, \mathbf{H}_{Ti}\, \ddot{\mathbf{y}}_{Ti} &= \mathbf{f}_i^{\,e}, \\ \mathbf{I}_i\, \mathbf{H}_{Ri}\, \ddot{\mathbf{y}}_{Ri} \ + \ \mathbf{I}_i\, \dot{\mathbf{H}}_{Ri}\, \dot{\mathbf{y}}_{Ri} \ &+ \boldsymbol{\omega}_i \times \mathbf{I}_i\, \boldsymbol{\omega}_i = \mathbf{l}_i^{\,e}. \end{aligned} \tag{1}$$

Here, $\mathbf{H}_{Ti}$ and $\mathbf{H}_{Ri}$ are the Jacobian matrices of translation and rotation, respectively. Since the translational degrees of freedom are uncoupled, $\mathbf{H}_{Ti}$ equals the 3×3 identity matrix, whereas $\mathbf{H}_{Ri}$ equals

$$\mathbf{H}_{Ri} \ = \ \begin{bmatrix} 1 & 0 & \sin\beta \\ 0 & \cos\alpha & -\sin\alpha\cos\beta \\ 0 & \sin\alpha & \cos\alpha\cos\beta \end{bmatrix}, \tag{2}$$

see [Schiehlen, Eberhard, 2004], and $\dot{\mathbf{H}}_{Ri}$ is the time derivative of the corresponding Jacobian matrix. The mass of each body and its inertia tensor are denominated by m_i and $\mathbf{I}_i$, respectively. The rotational degrees of freedom for each body are summarized in $\mathbf{y}_{Ri}$, where we have

$$\boldsymbol{\omega}_i \ = \ \mathbf{H}_{Ri}\, \dot{\mathbf{y}}_{Ri} \tag{3}$$

for the rotational velocity. Finally, $\mathbf{f}_i^{\,e}$ and $\mathbf{l}_i^{\,e}$ of Equation (1) are the forces and moments, that are acting on each body due to gravity and contact.

4 Neighborhood Search

For a system consisting of n bodies, the required calculation operations for naive collision detection will be of order $O(n^2)$, causing great computational effort. However, there exist special neighborhood search algorithms, so that a tremendous reduction of the computational effort down to the order $O(n)$ can be achieved, [Allen, Tildesley, 1989]. The neighborhood search method we want to use here, the Linked Linear List (LLL), is described e.g. in [Schinner, 1999]. Every body whose bounding box is colliding with the bounding box of another particle is considered to be a neighbor of this body. Therefore, in a first step, bounding boxes are laid around each particle, see Figure 1, that are sized in such a way, that each particle fits exactly in its box. The edges of each bounding box are aligned with the coordinate axes. In a next step the bounding boxes are projected separately onto the system axes. Such a projection onto the x-axis is shown in Figure 1. In the following, only the order of the beginnings and endings of the projections of the bounding boxes along the axes is of interest. These beginnings and endings are identified here by a negative and positive value, respectively. The resulting sequences are stored in lists.

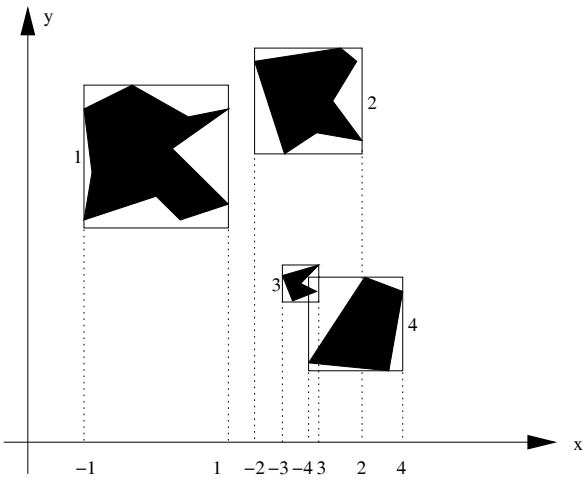

Figure 1. Bounding boxes projected to the x-axis.

Each of these lists, therefore, has a length which corresponds to twice the number of particles in the system. If there is the beginning, ending, or both, of another particle in between the beginning and ending of a particular body, then there will be an overlap of the projections of the bounding boxes for these two particles along the axis. A collision of two bounding boxes exists for an overlap of these projections along all axes. Checking whether there is some part of a projection in between the beginning and ending of another projection for each particle along each axis still takes a lot of time. But, although these lists have to be updated for each time step, the necessary calculation times can be reduced to an amount proportional to the total number of particles in the system, as there has to be done only an update of the old list for each new time step. This corresponds to sorting an already nearly sorted list, which can be done with an effort of $O(n)$. This update can simply be done by going sequentially through the lists and checking for any new changes in the order. The occurring changes are usually permutations only. If the order of the beginnings and endings does not have to be changed, the collision status of the particles also will remain unchanged. While seeking for new colliding bounding boxes by looking for permutations in the lists, four different cases have to be discerned. If two beginnings or two endings are changing their order, the collision status of the two bodies will remain unchanged. If a beginning and a proximate ending have changed, a previously occurring overlap has to be removed. Finally, if an ending and a following beginning of another particle are exchanged, then a previously non-existing overlap has to be taken into account now. If a collision along an axis has to be removed, or if there is a new collision between two particles along an axis, the collision information along the other axes is essential and has to be compared.

The bodies, whose bounding boxes collide along all system axes, are called neighbors here. Each neighboring body-pair is now stored within a new list, called the LLL and checked further in the collision detection.

5 Collision Detection

As soon as neighboring body pairs are sorted, the even more time consuming collision detection can be carried out. It only has to be carried out for body-pairs that are stored in the LLL. For these body-pairs, it is necessary to check, whether and which surface points of the bodies are located inside another body. That means, for each neighboring body pair (e.g. body pair 3 and 4 in Figure 1) it has to be checked, whether vertices of polyhedron 3 lie within 4 and vice versa. In order to check, whether a point $\mathbf{q}$ is positioned within another body, e.g. the body of Figure 2, a ray originating from the observed point is created. Then the intersections of this ray with the surface of the body are counted, see [O'Rourke, 1993]. Point $\mathbf{q}$ is inside the other body, if the number of intersections with the surface of the other body is odd for all possible rays. Also it can be said, that the point is outside the other body, if the number of intersections is even for all rays from this point (where 0 is considered to be an even number). In order to check that, the ray has to be tested against all separate surface parts of the body, and for that purpose, to all planes around the surfaces. By controlling, whether an intersection point of the ray with the plane of a surface really lies on the surface of the body, the rate of distance 1, (which is the distance between the observed point to the surface) to distance 2 (that is the distance of a point of the ray that is clearly located outside the body to the surface) has to be considered. If that rate equals zero, that means point $\mathbf{q}$ equals the point of intersection of the ray with that observed surface and, therefore, point $\mathbf{q}$ is positioned directly on the surface of the body, see [O'Rourke, 1993; Wessel, 2004]. These considerations have to be taken into account for each surface point of both neighboring bodies.

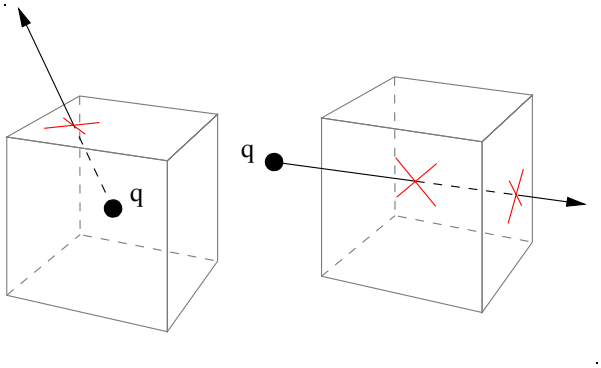

Figure 2. Collision detection by means of a ray through the bodies.

6 Contact Force Calculation

Since the investigated bodies here are solids, interactions between bodies are due to measurable properties of the bodies and their material such as viscosity, elasticity, friction, and so on. These interactions are leading to contact forces. They can be divided into normal contact forces and tangential contact forces.

6.1 Contact Force in Normal Direction

For the calculation of the contact forces in normal direction a penalty-formulation is used, i.e. overlaps between the bodies are accepted, and the size of the contact force is dependent on this overlap. The contact forces are then calculated by means of the Calvin-Voigt model, [Lankarani, Nikravesh, 1994]. There, the contact force is consisting of an elastic and a viscous part. The elastic part shows a direct relationship between the elastic contact force and the overlap of the two bodies. The absolute value of the viscous part may not be larger than the elastic part, since the total value of the contact force could then become negative for negative relative velocity. Therefore, the viscous part of the contact force is dependent on the overlap as well. The contact force in normal direction can then be written as

$$\mathbf{f}_N = \underbrace{K\delta^n\,\mathbf{n}}_{\text{elastic force}} + \underbrace{K\delta^n\,\frac{3\,(1-e^2)}{4}\,\frac{\dot{\delta}}{\dot{\delta}_{\text{beg}}}\,\mathbf{n}}_{\text{viscous force}}. \quad (4)$$

Here, δ and $\dot{\delta}$ are the overlap between the two bodies and their relative velocity at the contact point, respectively. The relative velocity at the beginning of the contact is denoted with $\dot{\delta}_{\text{beg}}$ and the coefficient of restitution is called e. That means, the damping coefficient d is here depending on the stiffness parameter K,

$$d = \frac{3\,K\,(1-e^2)}{4\,\dot{\delta}_{\text{beg}}} \quad (5)$$

which leads to a total relative kinetic energy change during the contact of

$$\Delta T = \frac{1}{2}\,m_{\text{eff}}\,\dot{\delta}_{\text{beg}}^2\,(1-e^2). \quad (6)$$

For a more detailed explanation of this see e.g. [Hunt, Grossley, 1975; Lankarani, Nikravesh, 1994].

6.2 Contact Force in Tangential Direction

For the tangential contact force, generally two phases can be distinguished. The friction process is then divided into a static sticking phase and a dynamic phase that can be called sliding or slipping, see [Cundall, Strack, 1979; Wriggers, 2002], respectively. The well-known Coulomb friction model distinguishes between sticking and sliding in such a way, that during sticking, no tangential motion is possible. The contact force during sticking is not given explicitly, but it has to fulfill the condition that no relative motion between the bodies can occur. The model leads to an undifferentiability. In order to avoid that, some authors introduced associated models, see e.g. [Oden, Pires, 1983; Wriggers, 2002], where the frictional contact force is based on a functional form which leads to a smooth transition from sticking to sliding. For instance, an $\arctan$-function is used sometimes. For these associated models, the friction force is dependent on the relative velocity between the contacting bodies,

$$\mathbf{f_t} = -\frac{\mathbf{v_t}}{\|\mathbf{v_t}\|}\min(k\|\mathbf{v_t}\|, \mu\mathbf{f_n}). \quad (7)$$

The problem with such a force law is however, that it leads to a contact force that is zero for no relative tangential velocity, and hence, e.g. a block on an inclined plane can never come to rest.

In the following, we want to use the Cundall-Strack model [Cundall, Strack, 1979]. That model also distinguishes between a sticking and a sliding phase, see

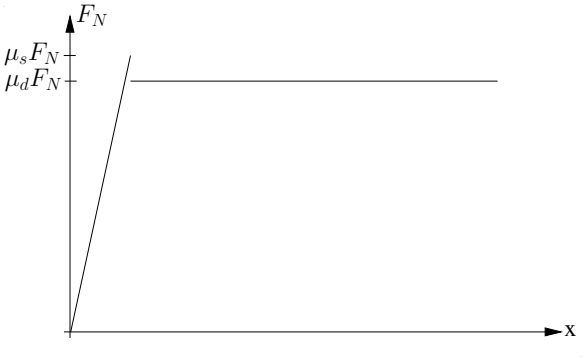

Figure 3. Friction force in the Cundall-Strack model.

Figure 3 and the contact force is not dependent on the relative velocity in the tangential plane but to its corresponding relative displacement,

$$\mathbf{f_t} = -\frac{\boldsymbol{\xi_t}}{\|\boldsymbol{\xi_t}\|}\min(k\|\boldsymbol{\xi_t}\|, \mu\mathbf{f_n}). \quad (8)$$

That means, it is the approach of this model that the friction force acts in opposite direction to a small tangential motion that is allowed here also in the sticking phase, due to surface roughness. The sticking force is then influenced by that tangential displacement in its direction and also in its value. In Figure 4 the tangential plane is shown. The figure shows a cut through the friction cone, i.e. a cut perpendicular to the normal direction at the level of the actual normal contact force $\mathbf{f}_N$ of Figure 3, see Figure 5. Therefore, the applied force is shown in this figure over the tangential plane. The circle shows the border between the sticking and the sliding zone, where sticking occurs inside and sliding outside. The beginning of the contact is at the origin of the coordinate system. In this example the line from 0 to 1 shows the tangential displacement of two bodies, $\boldsymbol{\xi}_{t1}$, due to some acting forces. Point 1 is clearly within the sticking zone. Therefore, the contact force that has

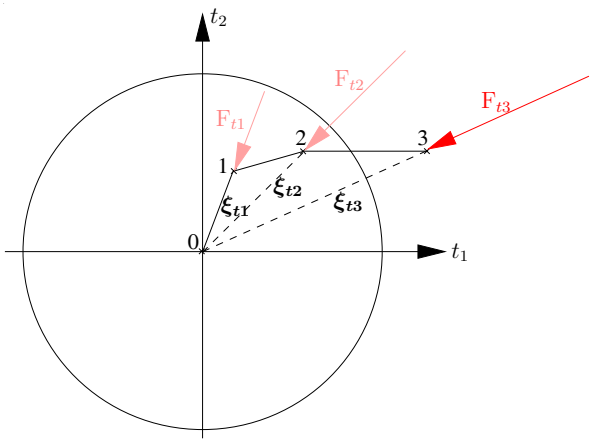

Figure 4. Cut of friction cone at actual normal force, parallel to the tangential plane.

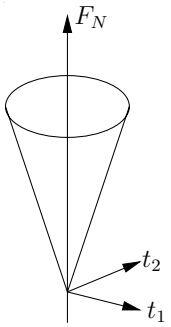

Figure 5. Three dimensional figure of the friction cone.

to be applied, $\mathbf{F}_{t1}$, is a sticking-force, its size being proportional to the distance between 0 and 1, see Figure 4. In a next time step, the tangential displacement may change, e.g., due to the impulse of another body in the system. Then the point, that is in contact, has moved and its projection onto the tangential plane is here, e.g., point 2. If this point is still within the circle, then still sticking occurs. The sticking force in this case is proportional on the tangential displacement $\boldsymbol{\xi}_{t2}$ in its total direction and value, see $\mathbf{F}_{t2}$ of Figure 4. That means, in each time step, the displacement $\boldsymbol{\xi}_t$ in tangential direction has to be re-calculated and added up vectorially. The force is then applied in opposite direction of that total displacement. As soon as sliding occurs, e.g. in the timestep from point 2 to 3, the value of the friction force will be restricted to the sliding force. That means, its magnitude is restricted to $\mu_d \mathbf{F}_N$ which corresponds to the radius of the circle. The direction of this force still changes with each time step but will always be directed to the origin of the tangential system.
If, in a later time step, when the contact still exists, the relative motion stops and changes its direction, a sticking force has to be applied to the bodies. By means of the conventional model, this is not possible, see [Brendel, Dippel, 1998]. If the elongation of $\boldsymbol{\xi}_t$, has been updated in each time step, after a long sliding phase it will take a long backwards motion in opposite direction to release this "spring". Therefore, [Brendel, Dippel, 1998] propose not to update the elongation of $\boldsymbol{\xi}_t$ during sliding, but to keep it constant, i.e. at the value that corresponds to the particular radius of the circle, until sticking occurs again. The solution for the contact force in a planar example is given in [Brendel, Dippel, 1998], and is extended here to a spatial statement,

$$\begin{aligned} \mathbf{f_t} &= -k_t \boldsymbol{\xi}_t, \\ \boldsymbol{\xi}_t &= \int_{t_0}^{t} \mathbf{v_t} \Theta \left(\frac{\mu \|\mathbf{f_n}\|}{k_t} - \|\boldsymbol{\xi}_t\| \right) dt', \end{aligned} \tag{9}$$

where $\Theta(\bullet)$ is the Heaviside function. Therefore, an update of $\boldsymbol{\xi}_t$ will only be carried out for $\mu \|\mathbf{f_n}\| > k_t \|\boldsymbol{\xi}_t\|$.

7 Comparison of the Friction Results

In the following, the example of a block on an inclined plane will be used in order to show its behavior, when friction is modeled by means of the Cundall-Strack model. The block, that is shown in Figure 6, has the volume of $0.001m^3$. With a density of $\rho = 2700\ kg/m^3$ its mass is $m = 2.7kg$. The angle of the inclined plane is $\alpha = 30°$ and the critical value for the friction coefficient is $\mu = \tan(\alpha) \approx 0.57735$. In Figure 7 the behavior of the block is shown for three different values of μ. The two lines at the top lie very closely together. It can be seen, that for $\mu > \tan(\alpha)$, the block does not slip off. The zoomed depiction of the behavior for $\mu = 0.58$ and $\mu = 0.6$ is shown in Figure 8. In both cases, the block oscillates slightly, but keeps its global position on the plane.

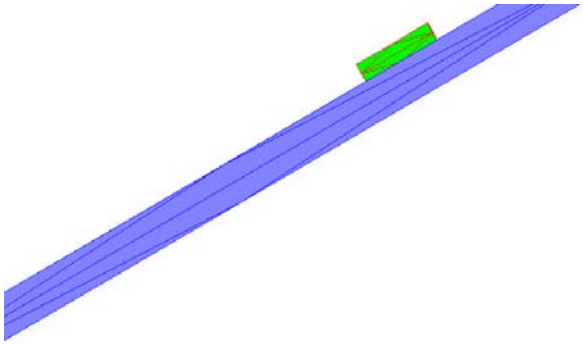

Figure 6. Block on top of an inclined plane.

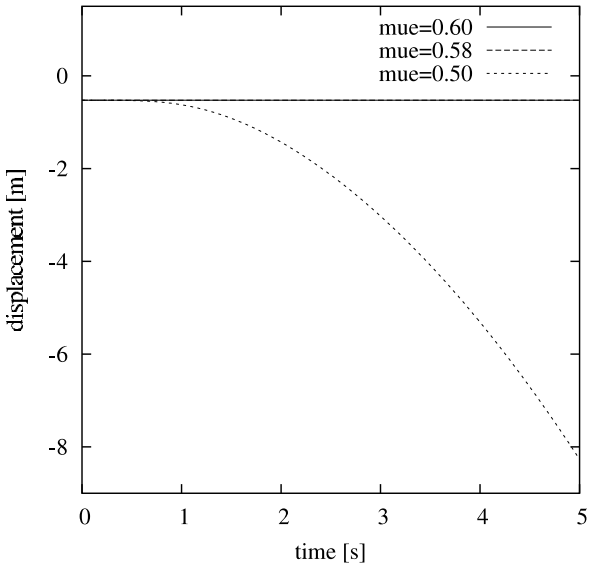

Figure 7. Stick-slip behavior for different friction coefficients in a simulation for 5 sec., motion in m.

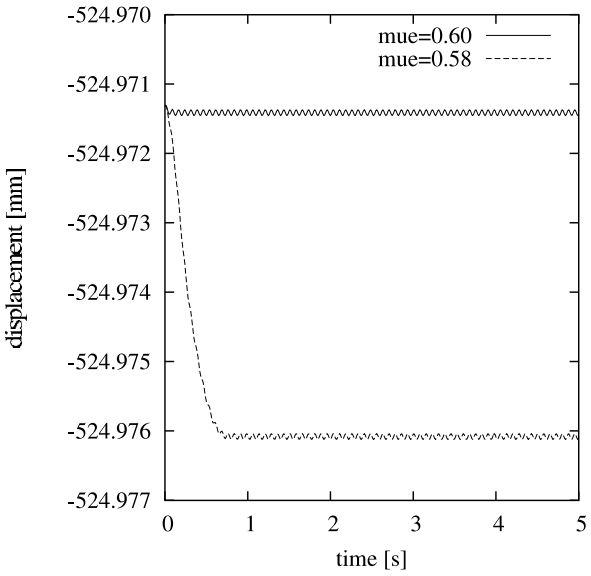

Figure 8. Zoomed stick-slip behavior for the large friction coefficients, motion in mm.

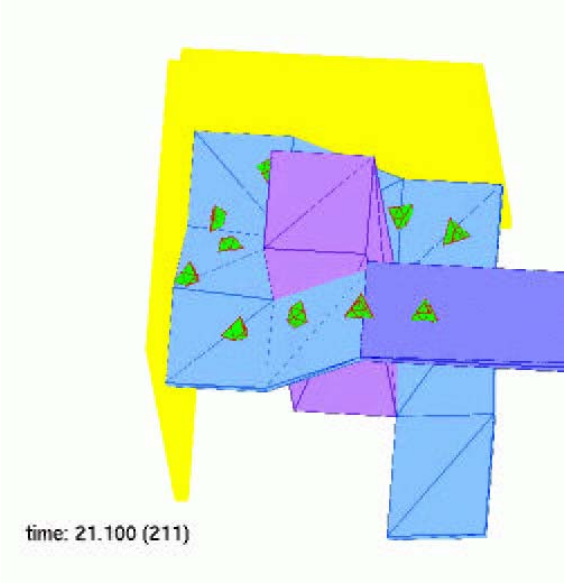

Figure 10. Top view of a helix containing granular material.

8 Example

The explained methods are applied to a simulation program in order to simulate granular material. We are mainly interested in particles which are larger than molecules, and appear e.g. in production processes in mechanical engineering. In the following, results from the motion of bulk solids inside a helix are shown. The particles have the shape of non-convex polyhedra. Here, a simulation with the total simulation time of $40s$ is carried out. In the beginning, the bodies are lined up on top of a bar, see Figure 9. An initial velocity is applied to the bodies such that the bodies are moving in direction to the helix. After reaching the helix, the bodies are falling and by means of the helix kept on a given course. The top view of that simulation at time $t = 21.1s$ is given in Figure 10. The side view of the same simulation at time $t = 29.7s$ is shown in Figure 11.

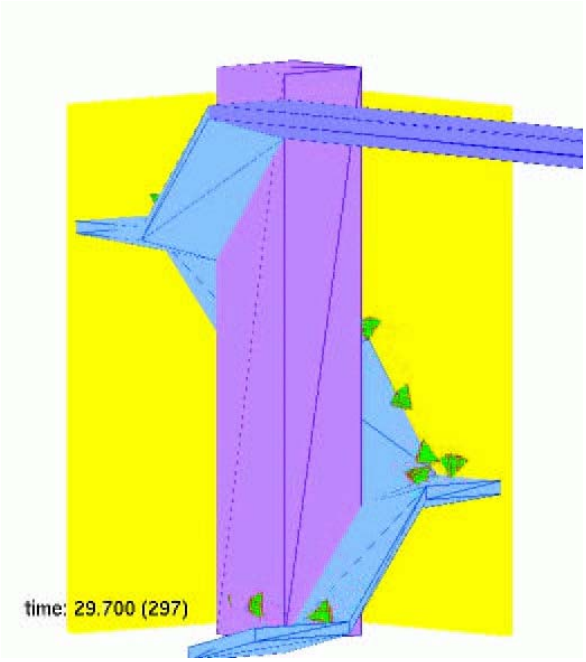

Figure 11. Side view of a helix containing granular material.

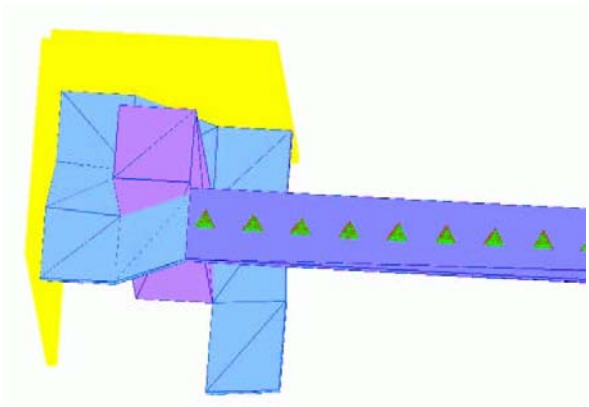

Figure 9. Initial condition for the simulation of a helix containing granular material.

9 Conclusion

In this paper we could show, that an efficient calculation of the dynamical behavior of many differently shaped bodies can be achieved by combining ideas from MD with MBS. In MD, the interactions and the collective dynamical behavior of molecules or other large systems are investigated. In order to simulate a high number of bodies, in MD the bodies are modeled as rigid. The material behavior is then represented by the forces acting on the bodies. In order to calculate contact forces effectively, overlaps between the particles are accepted and the value of the contact force depends on the distance between the colliding bodies. Another concept, which was used, is the neighborhood

search. By means of that method it is possible to search for close body pairs in advance and to evaluate the necessary contact forces only for the colliding body pairs. By means of such neighborhood search methods it is possible to reduce the necessary simulation time of order $O(n^2)$ in such a way that a linear behavior $O(n)$ can be obtained.

The equations of motion could be obtained easily, since simulations of granular material or bulk solids are based on free bodies in space. The very time consuming collision detection only had to be carried out for neighboring body pairs. For colliding bodies, the contact force calculation was conducted. The calculation of the contact forces in normal direction was modeled by means of the Calvin-Voigt model. For the modeling of the tangential contact force, the Cundall-Strack model was used. There, the friction force is modeled dependent on the relative displacement between two contacting bodies. By means of that model it could be shown, that a block on an inclined plane can stay there, without slipping off. Finally, an example of bodies within a helix was presented. It is our goal to examine the dynamical behavior of practical applications by means of such simulations.

References

Allen, M.P. and Tildesley, D.J. (1989). *Computer Simulations of Liquids*. Clarendon Press. Oxford.

Brendel, L. and Dippel, S. [1998]. Lasting Contacts in Molecular Dynamics Simulations. *Physics of Dry Granular Materials, NATO ASI Series*, **E350**, pp. 313-318.

Cundall, P.A. and Strack, O.D.L. [1979]. A Discrete Numerical Model for Granular Assemblies. *Geotechnique*, **29**(1), pp. 47-65.

Eberhard, P. (2000). *Kontaktuntersuchungen durch hybride Mehrkörpersystem / Finite Elemente Simulationen* (in German). Shaker Verlag. Aachen.

Hunt, K.H. and Grossley, F.R.E. [1975]. Coefficient of Restitution Interpreted as Damping in Vibroimpact. *ASME Journal of Applied Mechanics*, **7**, pp. 440-445.

Lankarani, H.M. and Nikravesh P.E. [1994]. Continuous Contact Force Models for Impact Analysis in Multibody Systems. *Nonlinear Dynamics*, **5**, pp. 193-207.

Luding, S. [1998]. Collisions and Contacts Between Two Particles. *Physics of Dry Granular Media, Nato ASI Series*, **E350**, pp. 285–304.

Oden, J.T. and Pires, E.B. [1983]. Nonlocal and Nonlinear Friction Laws and Variational Principles for Contact Problems in Elasticity. *Journal of Applied Mechanics*, **50**, pp. 67–76.

O'Rourke, J. (1993). *Computational Geometry in C*, (2. Edition). Cambridge University Press. Cambridge.

Schiehlen, W. and Eberhard, P. (2004). *Technische Dynamik* (in German). Teubner. Stuttgart.

Schinner, A. [1999]. Fast Algorithms for the Simulations of Polygonal Particles. *Granular Matter*, **2**(1), pp. 35–43.

Schwertassek, R. and Wallrapp, O. (1999). *Dynamik flexibler Mehrkörpersysteme* (in German). Friedr. Vieweg & Sohn. Braunschweig.

Wessel, W. (2004). *Kontakterkennung räumlicher polyhedraler Körper mit Hilfe von Methoden der Molekulardynamik* (in German). Student-Thesis, **STUD-212**. Institute B of Mechanics, University of Stuttgart. Stuttgart.

Wriggers, P. (2002). *Computational Contact Mechanics*. John Wiley & Sons. Chichester.